Potential of green-synthesized ZnO NPs against human ovarian teratocarcinoma: an in vitro study

Potential of green-synthesized ZnO NPs against human ovarian teratocarcinoma: An *in vitro* study

Mohd Shahnawaz Khan*[1], Nojood Altwaijry[1], Nasimudeen R. Jabir[2], Abdulaziz Mohammed Alamri[1], Mohammad Tarique[3], Azhar U. Khan[4]

[1]Department of Biochemistry, College of Sciences, King Saud University, Riyadh, 11451, Saudi Arabia

[2]Department of Biochemistry and Biotechnology, Centre for Research and Development, PRIST University, Vallam, Thanjavur, 613403, Tamil Nadu, India

[3]Department of Child Health, University of Missouri, Columbia, USA

[4]Department of Chemistry, School of Life and Basic Sciences, SIILAS CAMPUS, Jaipur National University, Jaipur, India

* **Address for correspondence:**

Dr. Mohd Shahnawaz Khan

Email: moskhan@ksu.edu.sa

Abstract

Background: Ovarian cancer leads to devastating outcomes, and its treatment is highly challenging. At present, there is a lack of clinical symptoms and well-known sensitivity biomarkers, and patients are diagnosed at an advanced stage. Currently, available therapeutics against ovarian cancer are inefficient, costly, and associated with side effects. The present study evaluated the anticancer potential of zinc oxide nanoparticles (ZnO NPs) that were biosynthesized successfully in an ecofriendly mode using pumpkin seed extracts. **Methods and Results**: The anticancer potential of the biosynthesized ZnO NPs was assessed using an *in vitro* human ovarian teratocarcinoma cell line (PA-1) by well-known assays such as MTT assay, morphological alterations, activation of apoptosis, measurement of reactive oxygen species (ROS) production, and inhibition of cell adhesion/migration. The biogenic ZnO NPs exerted a high level of cytotoxicity against PA-1 cells. Furthermore, the ZnO NPs inhibited cellular adhesion and migration but induced ROS production and cell death through programmed cell death. **Conclusions**: The aforementioned anticancer properties highlight the therapeutic utility of ZnO NPs in ovarian cancer treatment. However, further research is recommended to envisage their mechanism of action in different cancer models and validation in a suitable *in vivo* model.

Keywords: Anticancer; biogenic ZnO NPs; cytotoxicity; nanomedicine; ovarian cancer

2

1. Introduction

Despite notable advancements in cancer-related research during the past few decades, cancer remains the major contributor to global mortality and imposes a substantial financial burden on the patient [1, 2]. Among the different cancer types, ovarian cancer (OC) is one of the fatal malignancies in women, with a reported frequency of approximately 15 per 100,000 cases, ranking third in incidence and first in mortality among all gynecological malignancies [3, 4]. These cancers always lead to devastating outcomes in women, and their treatment is highly challenging [5-7]. Because of the lack of clinical symptoms and well-known sensitivity biomarkers, patients with OC are often diagnosed at an advanced stage, which significantly worsens the clinical outcome and considerably limits therapeutic options [8]. OC is detected in more than 75% of women at stage III or IV, with 5- and 10-year survival rates of 5% and 21%, respectively [9]. These data indicate the limited efficacy of existing drugs and highlight the need for novel therapeutic strategies to combat or manage OC. Furthermore, the non-selectivity of the drug and the inability to release the drug at the target tumor site are the primary therapeutic obstacles [10].

Despite the overall favorable response to surgical excision and intravenous chemotherapy with platinum/taxanes, the treatment is still difficult in advanced stages [11, 12]. Although many cytotoxic and synthetic medications have been tried as first-line therapies, they haven't demonstrated any appreciable survival improvements [13]. They are linked to negative side effects, recurrence risk, and treatment resistance. For better survival, it is critically necessary to develop new treatments for ovarian cancer, and it is crucial to conduct research to identify effective therapeutic options and novel administration routes.

Multifunctional nanoparticles have great potential for use in cancer treatment and can overcome the limitations of conventional therapy [14]. Nanoparticles (NPs) have great therapeutic potential owing to their high surface area-to-volume ratio, considerably smaller size, ability to permit tumor cells to bind with many functional groups, and potential to accumulate at tumor sites [15, 16]. Recently, plant products have been exploited for the synthesis of NPs because of their eco-friendly and cost-effective nature [17, 18]. Metal oxide NPs are an appealing alternative for synthesizing a robust drug-delivery platform because they can be functionalized with various chemical groups, which allows them to bind to multiple therapeutic ligands [19-21].

Zinc oxide, one such metal oxide, has shown potency as an antibacterial agent, with a higher potency being observed in its nanoform [22]. Zinc oxide NPs (ZnO NPs) have attracted attention

3

and are widely used in various applications, including textiles, cosmetics, diagnostics, and micro-electronics [23]. Their clinical significance is attributed to their strong potential and decisiveness when compared with other metal oxide NPs prepared through the green synthesis method [24]. The wide band gaps, high excitation binding energy, exceptional photosensitivity, and stability of the ZnO NPs have garnered the attention of scientists working in this field of research globally. Compared with physical and chemical processes, green-synthesized ZnO NPs have various advantages, namely, low cost, eco-friendly nature, biosafety, non-toxicity, and biocompatibility, and have therefore been widely used in various biomedical applications [25, 26]. In our previous study, we reported the biogenic synthesis and characterization of ZnO NPs [22]. The present study aimed to evaluate the anticancer potential of the ZnO NPs biosynthesized from pumpkin seed extracts in an OC model. The present work is an extension of our previous study, and we focus on determining the best responsive cancer model so that our novel nanoformulation could be validated in a suitable *in vivo* system and further applied in the clinical setting.

2. Materials and methods

The chemicals used in all the experiments were bought commercially from Merck and Sigma, which are as follows: Trypsin-EDTA, streptomycin, penicillin, phosphate-buffered saline (PBS), 3-(4,5 dimethylthiazol-2-yl)-2,5-diphenyltetrazolium bromide (MTT), 2′7′-dichlorofluorescein diacetate (DCFH-DA), acridine orange (AO), and ethidium bromide (EtBr). All other chemicals were of analytical grade and were purchased locally.

2.1. Synthesis and characterization of ZnO NPs

The production of ZnO NPs was confirmed using ultraviolet-visible (UV-Vis) spectroscopy; a peak at 272 nm indicated the biosynthesis of ZnO NPs. Several spectral techniques such as Fourier transform infrared (FTIR) spectroscopy, scanning electron microscopy (SEM), transmission electron microscopy (TEM), X-ray diffraction (XRD), and energy-dispersive X-ray spectroscopy were also used for further characterization of the ZnO NPs.

2.2. Cell culture maintenance

The National Centre for Cell Science in Pune, India, provided the ovarian teratocarcinoma cell line (PA-1). The cell line was cultured in high-glucose Dulbecco's Modified Eagle Medium (DMEM), which was supplemented with 10% fetal bovine serum (Gibco, USA), penicillin (100 U/mL), and streptomycin (100 µg/mL) in a humid atmosphere. The growth conditions were 37 °C and 5% CO2.

2.3. Cytotoxicity (MTT) assay

MTT test was used to measure the cytotoxicity of ZnO NPs on PA-1 cells after they were exposed to various concentrations (2.5–17.5 µg/mL). After incubation, 10 µL of MTT was added to each well, and the plate was then incubated for 2 hours at 37 °C. After mixing in 100 µL of dimethyl sulfoxide to dissolve the purple precipitate containing formazan, the absorbance at 540 nm was measured using a multi-well plate reader.

To determine the cytotoxicity of ZnO NPs, the percentage of viable cells was counted and compared with the control cells, according to the following formula:

Inhibitory of cell proliferation (%)

= (mean absorbance of the control − mean absorbance of the sample)/(mean absorbance of the control) × 100

The 50% inhibitory concentration (IC_{50}) was determined using ZnO NPs dose-responsive curve.

2.4. Measurement of apoptosis activation

Fluorescence microscopic assessment of programmed cell death was performed according to the method described in Tabrez et al. [27]. Each well of a 6-well plate was seeded with 5×10^4 PA-1 cells, which were then exposed to various concentrations of ZnO NPs (7.5, 10, and 12.5 µg/mL) for 24 hours. The cells were then washed with cold PBS and stained for 5 min with AO/EtBr (1:1 ratio; 100 µg/mL), before being examined under a fluorescence microscope (40× magnification).

The proportion of cells undergoing apoptosis was calculated over the total number of cells. A graph was plotted with the concentration of ZnO NPs on the X-axis and the percentage of apoptotic cells on the Y-axis.

2.5. Measurement of reactive oxygen species

Reactive oxygen species (ROS) were measured using a dichloro-dihydro-fluorescein diacetate (DCFH-DA) fluorogenic probe as earlier reported [21]. The treated cells were first washed with PBS and then allowed to react with 25 µM of DCFH-DA for 30 min at 37 °C. Finally, DMEM was used to wash the cells, and their fluorescence was recorded using a spectrofluorometer (excitation wavelength: 485 nm, emission wavelength: 535 nm; Shimadzu, Columbia, USA) every 5 min for up to 30 min. The mean slope per minute, normalized to the exposed control cells, was used to calculate the increase in ROS production.

5

2.6. Cell adhesion assay

Cells were first cultured in 6-well plates and then divided at 0, 15, 30, 45, and 60 min. The cells were washed with PBS to remove cells that were weakly adhered or completely unattached. Crystal violet dye was added to 5% paraformaldehyde to fix the seeded cells, and the mixture was then let to sit for 15 minutes to allow the dye to bind to the proteins of the cells. After 15 min of incubation, the extra dye was removed by washing the cells with PBS. The amount of crystal violet that was de-stained from the protein was inversely correlated with the number of cells in the well.

2.7. In vitro scratch assay

A sterile 200-µL micropipette tip was used to scratch (by drawing a straight line) the adherent cells. Subsequently, the cells were exposed to various concentrations of ZnO NPs (7.5, 10, and 12.5 µg/mL). After two washes with PBS, the cells were incubated for 24 h at 37 °C and 5% CO_2. Wound width was measured at four new specific areas after 0 and 24 h. At reference areas, the distance between the two edges of the wound was calculated and statistically examined.

2.8. Statistical analysis

The quantitative estimation data are expressed as mean ± SD with at least two independent experiments performed in triplicate and analyzed by one-way ANOVA using Graph Pad Prism software version 5 (San Diego, CA). $P < 0.05$ was considered statistically significant.

3. Results

3.1. Synthesis and characterization of ZnO NPs

The reduction of Zn^{2+} to ZnO resulted in a color shift from light yellow to cream, confirming the formation of ZnO NPs, with a characteristic stable UV-vis spectral peak at 272 nm. Various spectral techniques, namely, FTIR, XRD, SEM, and TEM analyses, were used for the characterization of ZnO NPs. As reported earlier, ZnO NPs showed a strong FTIR stretching vibration frequency at around 671–482 cm^{-1} and a peak in the range of 500–4000 cm^{-1}. XRD analysis of ZnO NPs revealed 2θ intensity peaks at 31.72°, 34.32°, 36.16°, 47.35°, 56.38°, 62.87°, and 67.91°, with Miller indices similar to the results of Wurtzite structure. Moreover, TEM data indicated the spherical and hexagonal shapes of ZnO NPs with a ~50 nm size.

3.2.Cytotoxicity assay (MTT) and morphological changes

When compared to untreated control cells, we observed a dose-dependent decrease in the viability of PA-1 cells with an increasing concentration of ZnO NPs (Figure 1). Our data suggest a linear decline in cell viability (increased cytotoxicity) with ZnO NP concentrations ranging from 2.5 µg/mL to 17.5 µg/mL. After 24 hours of treatment with ZnO NPs, cell viability began to decline at the lowest tested concentration (2.5 µg/mL) and decreased up to 18.8% at the highest tested concentration (17.5 µg/mL). When we draw the dose-response curve, the biosynthesized ZnO NPs were found to have an IC_{50} concentration of 10 µg/mL Based on the IC_{50} value, we selected three different concentrations (7.5, 10, and 12.5 µg/mL) of ZnO NPs for the subsequent experiments. As for morphological changes in PA-1 cells in response to different concentrations of ZnO NPs after 24 h of treatment, the cells showed shrinkage, detachment, membrane blebbing, and distorted shape (Figure 2). However, the cell morphology of the untreated cells was normal and intact (10× magnification). Moreover, maximum alteration in the morphological characteristics of PA-1 cells was observed at the highest concentration of ZnO NPs.

3.3. ZnO NPs induced apoptosis in PA-1 cells

The AO/EtBr fluorescence pattern of PA-1 cells treated with ZnO NPs revealed the presence of apoptotic cells at both early and late stages of cell death (Figure 3), implying apoptosis induction by ZnO NPs. Most of the untreated/control cells had intact and normal nuclear membrane. However, the number of early-stage apoptotic cells with nuclear fragmentation significantly enhanced as the concentration of ZnO NPs increased from 7.5 to 12.5 µg/mL. Furthermore, the increase in nuclear fragmentation could be a sign of cells reaching the advanced stage of apoptosis (Figure 3). We also quantified the percentage of apoptotic cells in each group and found that the highest percentage of apoptosis (80.9%) was obtained with the highest concentration of ZnO NPs (Figure 4).

3.4. ZnO NPs induced intracellular ROS generation in PA-1 cells

Treatment with ZnO NPs resulted in high levels of ROS in PA-1 cells. As shown in Figure 5, treatment with different concentrations of ZnO NPs (7.5, 10, and 12.5 µg/mL) produced high levels of ROS when compared with those in untreated control cells. Our data suggested a dose-dependent increase in intracellular ROS production, which subsequently induced oxidative stress and enhanced DCFH fluorescence intensity in the treated PA-1 cells. Untreated control cells showed a dull green fluorescence, whereas ZnO NP-treated cells showed a strong DCF-stained green fluorescence (Figure 5). To quantify the relative fluorescence intensity, the cells were lysed after capturing images and normalizing with protein concentrations. The fluorescence intensity for ROS production showed an increasing trend with an increasing concentration of ZnO NPs (Figure 6).

3.5. Effect of ZnO NP treatment on cell adhesion in PA-1 cells

Treatment with ZnO NPs suppressed cell growth and adherence of PA-1 cells when compared with those of untreated control cells (Figure 7).

7

3.6. Effect of ZnO NP treatment on cellular migration in PA-1 cells

Treatment with different concentrations of ZnO NPs (7.5, 10, and 12.5 µg/mL) delayed the complete closure of the scratched area after 24 h, leading to decreased motility and migration of cancer cells (Figure 8). This test demonstrated that ZnO NPs have a beneficial inhibitory effect on cell migration. By comparing the leftover scar areas after 24 hours and edge progression to the starting gap area, the relative inhibition was measured. After 24 h of incubation, untreated control cells showed initiation of wound healing and migrated completely. However, the least cell movement and non-closure of the gap were observed at the highest tested concentration (12.5 µg/mL) of ZnO NPs (Figure 8).

4. Discussion

Recently, plant molecules and plant-based nanotherapeutics have been recognized as potential tool in cancer treatment and management [28-31]. The eco-friendly nature and biocompatibility of ZnO NPs, synthesized using various biological sources, have shown anticancer potential in different cancer models [22, 32-34]. Owing to the multifunctional properties of ZnO NPs, we conducted the present study as an extension of our previous study to determine the best responsive cancer model. This approach will aid in assessing the potential of our biogenic formulation so that the data can be validated in a suitable *in vivo* system and further applied in the clinical setting. The detailed procedure of the synthesis and characterization of ZnO NPs has been reported in our previous study [22]. Compared with other NPs, ZnO NPs hold several therapeutic advantages, including high bioavailability and solubility [35]. Additionally, they are more biocompatible than metal oxide NPs, can be easily synthesized, and have high selectivity [22, 36]. Interestingly, ZnO NPs are often more cytotoxic than other metal oxide NPs in various cancer types [37, 38]. Thatoi et al. reported a higher anti-inflammatory effect of ZnO NPs than that of AgNPs [39]. ZnO NPs have shown better anticancer activity at a comparatively lower concentration in various cancer cell lines. An IC_{50} dose of 10 µg/mL for ZnO NPs against PA-1 cells was the lowest concentration applied in the present study when compared with the dose of other metal oxide NPs such as MgO NPs (12.5 µg/mL against PA-1 cancer cells) and CuO NPs (20 µg/mL and 25 µg/mL against MDA-MB-231 and HCT-116 cells, respectively) [20, 21, 27].

Cytotoxicity potential is an essential aspect of an anticancer therapeutic candidate [40, 41]. The current study evaluated the cytotoxicity potential of ZnO NPs using the MTT assay and observed a significantly higher cytotoxic effect of the NPs in PA-1 cells that were treated with an increasing concentration of ZnO NPs than that in the untreated control cells (Figure 1). Our results agree with those of several published reports that assessed the cytotoxic potential of ZnO NPs in various cancer cell lines [32-34]. However, our biogenic nanoformulation showed a comparatively lower IC_{50} dose (10 µg/mL) against PA-1 cells. The release of zinc into the cell culture medium with the aid of CO_2 in the cell culture atmosphere is suggested as one reason for the observed cytotoxicity of ZnO NPs [42]. Moreover, the high solubility and oxidative stress-promoting ability of ZnO could have facilitated the cytotoxic effects [43]. ZnO NPs breakdown, which leads in the formation of Zn^{2+} ions, is what makes them toxic [43, 44]. Excess Zn^{2+} in the medium can alter the ionic equilibrium in the cells, resulting in the inhibition of ion transport and disturbance of amino acid metabolism [45].

The structural morphology of the treated cells as a monolayer showed shrinkage, detachment, membrane blebbing, and distorted shape induced by ZnO NPs at different concentrations (Figure 2). However, untreated control cells showed normal intact morphology. Exposure to green-synthesized ZnO NPs potentially promotes alterations in cellular morphology [22, 46, 47]. Cheng et al. evaluated the microscopic structural changes in MG-63 osteosarcoma cells after treatment with green-synthesized ZnO NPs [47]. In another study, typical morphological alteration in human breast cancer cells (MCF-7) was observed after exposure of the cells to ZnO NPs [46].

Effective destruction of cancer cells through induced apoptosis has been a hallmark and goal of clinical cancer therapy [48]. In the current study, we performed dual staining with AO and EtBr and used this method as a reliable tool to ascertain programmed cell death; the results showed hallmarks of apoptotic cells, including cell shrinkage, chromatin cleavage, nuclear condensation, nuclear disintegration, and the appearance of pyknotic structures, among others [49].

In the present study, PA-1 cells treated with ZnO NPs displayed early and late apoptosis. Nuclear material fragmentation, a morphological alteration of the treated cells, suggests possible induction of apoptosis [50]. Moreover, the presence of apoptotic cells further validated the cytotoxic potential of ZnO NPs in PA-1 cells. Recently, Boskabadi et al. reported that green-synthesized ZnO NPs were a natural apoptosis inducer [51]. ZnO NPs can also induce programmed cell death through different mechanisms [52, 53].

ROS is considered as a potent and promising target for the treatment of cancer and a significant contributing component to the induction of apoptosis through the intrinsic or extrinsic pathway [54]. Earlier studies reported the association of ROS with apoptosis induction and survivability of cancer cells [55, 56]. In the present study, cells treated with ZnO NPs exhibited a significant dose-dependent increase in the intracellular production of free radicals. Several research findings concur with ours, which states that one of the primary cytotoxicity pathways of green-synthesized ZnO NPs is an increase in ROS generation [23, 34, 57]. These results also suggest the potential of ZnO NPs to induce ROS production, which is otherwise reported as a second messenger for the induction of apoptosis and the associated cellular signaling pathways [58].

Cell adhesion is a critical process in several biological phenomena, such as cell development, tissue structure maintenance, angiogenesis, and tumor metastasis. When unattached, cancer cells cannot proliferate and undergo programmed cell death [59] . As cancer cell adhesion and migration are critical processes in metastasis, restricting these processes could be a therapeutic approach to prevent tumor development and metastasis [60, 61]. In the present study, we observed a gradual decrease in the adhesive PA-1 cell count with an increasing concentration of ZnO NPs (Figure 7). ZnO NP treatment caused a decline in the ability of PA-1 cancer cells to form colonies and attach to the substrate when compared with untreated control cells. All these results suggest the possible role of ZnO NPs in disrupting cellular interactions with the extracellular matrix and blockage of the tumor cell adhesion process. Cell migration and invasion are notable traits of cancer progression to metastasis. To evaluate the anti-migration ability of ZnO NPs, we performed the scratch wound assay, which measures cell migration ability in two dimensions and examines the anti-migration capacity of anticancer drugs without causing cell death [62]. This assay showed a generally positive trend in the inhibitory ability of ZnO NPs (Figure 8), which was consistent with the anti-migration ability of biogenic AgNPs and AuNPs in HCT-116 and MCF-7 cell lines [30, 63].

5. Conclusion:

The particular cell line-based study and our inability to make a quantitative estimation for some of the experiments are the limitations of this study. However, biogenic ZnO NPs seems to be a promising nanoformulation owing to their applicability in various biomedical applications. In the ovarian teratocarcinoma cell line (PA-1), the biosynthesized ZnO NPs demonstrated considerable cytotoxicity, apoptotic induction, enhanced ROS production, and inhibition of cell migration in PA-1 cells, which highlight their anticancer potential. However, more research in different *in vitro* models is recommended to determine the best responsive cancer type and further validate observed data in a suitable *in vivo* model before its application in the clinical setting.

6. Availability of data and material

Data will be available upon request to the corresponding author.

10

7. Consent to participate

Not applicable.

8. Consent to publish

All authors have given their consent to publish this research article.

9. Author contributions

NA, AMA, and MS conceived, designed, and guided this work. NRJ, AK, and MT executed the work, did the statistical analysis, and made this article's first draft. All authors reviewed the final draft of the manuscript.

10. Ethical approval

Not applicable

11. Declaration of Competing Interest

The authors declare that they have no known competing financial interests or personal relationships that could have influenced the work reported in this paper.

12. Acknowledgments

MSK acknowledges the generous support from the Research Supporting Project (RSP2023R352) by the King Saud University, Riyadh, Kingdom of Saudi Arabia.

11

13. References

1. Siegel RL, Miller KD, Fuchs HE, Jemal A.(2022) Cancer statistics, 2022. CA: A Cancer Journal for Clinicians.72(1):7-33. doi: 10.3322/caac.21708.

2. Tabrez S, Jabir NR, Khan MI, Khan MS, Shakil S, Siddiqui AN, et al.(2020) Association of autoimmunity and cancer: An emphasis on proteolytic enzymes. Seminars in Cancer Biology.64:19-28. doi: 10.1016/j.semcancer.2019.05.006.

3. Bhattacharya S, Anjum MM, Patel KK.(2022) Gemcitabine cationic polymeric nanoparticles against ovarian cancer: formulation, characterization, and targeted drug delivery. Drug Delivery.29(1):1060-74. doi: 10.1080/10717544.2022.2058645.

4. Joachim C, Véronique-Baudin J, Desroziers L, Chatignoux É, Belliardo S, Plenet J, et al.(2020) Gynaecological cancer in Caribbean women: data from the French population-based cancer registries of Martinique, Guadeloupe and French Guiana (2007–2014). BMC Cancer.20(1):643. doi: 10.1186/s12885-020-07128-1.

5. Gatenby RA, Brown JS.(2020) Integrating evolutionary dynamics into cancer therapy. Nat Rev Clin Oncol.17(11):675-86. doi: 10.1038/s41571-020-0411-1.

6. Shen S-F, Zhu L-F, Liu J, Ali A, Zaman A, Ahmad Z, et al.(2020) Novel core-shell fiber delivery system for synergistic treatment of cervical cancer. Journal of Drug Delivery Science and Technology.59:101865. doi: 10.1016/j.jddst.2020.101865.

7. Annaji M, Poudel I, Boddu SHS, Arnold RD, Tiwari AK, Babu RJ.(2021) Resveratrol-loaded nanomedicines for cancer applications. Cancer Rep (Hoboken).4(3):e1353. doi: 10.1002/cnr2.1353.

8. Piktel E, Ościłowska I, Suprewicz Ł, Depciuch J, Marcińczyk N, Chabielska E, et al.(2021) ROS-Mediated Apoptosis and Autophagy in Ovarian Cancer Cells Treated with Peanut-Shaped Gold Nanoparticles. Int J Nanomedicine.16:1993-2011. doi: 10.2147/IJN.S277014.

9. Ashihara K, Terai Y, Tanaka T, Tanaka Y, Fujiwara S, Maeda K, et al.(2020) Pharmacokinetic evaluation and antitumor potency of liposomal nanoparticle encapsulated cisplatin targeted to CD24-positive cells in ovarian cancer. Oncol Lett.19(3):1872-80. doi: 10.3892/ol.2020.11279.

10. Yokoe I, Omata D, Unga J, Suzuki R, Maruyama K, Okamoto Y, et al.(2021) Lipid bubbles combined with low-intensity ultrasound enhance the intratumoral accumulation and antitumor effect of pegylated liposomal doxorubicin in vivo. Drug Delivery.28(1):530-41. doi: 10.1080/10717544.2021.1895907.

11. Jaaback K, Johnson N, Lawrie TA.(2016) Intraperitoneal chemotherapy for the initial management of primary epithelial ovarian cancer. Cochrane Database Syst Rev.2016(1):CD005340. doi: 10.1002/14651858.CD005340.pub4.

12. Mammadova J, Redden A, Cruz R, Ujhazi B, Ellison M, Gatewood T, et al.(2022) Case Report: Initial Treatment Adjustments and Complications in Ovarian Cancer Patient With Inborn Error of Immunity. Frontiers in Oncology.12:843741. doi: 10.3389/fonc.2022.843741.

12

13. Nazam N, Jabir NR, Ahmad I, Alharthy SA, Khan MS, Ayub R, et al.(2023) Phenolic Acids-Mediated Regulation of Molecular Targets in Ovarian Cancer: Current Understanding and Future Perspectives. Pharmaceuticals.16(2):274. doi: 10.3390/ph16020274.

14. Zhao M-D, Li J-Q, Chen F-Y, Dong W, Wen L-J, Fei W-D, et al.(2019) Co-Delivery of Curcumin and Paclitaxel by "Core-Shell" Targeting Amphiphilic Copolymer to Reverse Resistance in the Treatment of Ovarian Cancer. Int J Nanomedicine.14:9453-67. doi: 10.2147/IJN.S224579.

15. Kumar N, Fazal S, Miyako E, Matsumura K, Rajan R.(2021) Avengers against cancer: A new era of nano-biomaterial-based therapeutics. Materials Today.51:317-49. doi: 10.1016/j.mattod.2021.09.020.

16. Tabrez S, Jabir NR, Adhami VM, Khan MI, Moulay M, Kamal MA, et al.(2020) Nanoencapsulated dietary polyphenols for cancer prevention and treatment: successes and challenges. Nanomedicine (Lond).15(11):1147-62. doi: 10.2217/nnm-2019-0398.

17. El-sonbaty SM, Moawed FSM, Kandil EI, M Tamamm A.(2022) Antitumor and Antibacterial Efficacy of Gallium Nanoparticles Coated by Ellagic Acid. Dose Response.20(1):15593258211068998. doi: 10.1177/15593258211068998.

18. Abuzenadah A, Al-Sayes F, Alam S, Hoque M, Karim S, Hussain I, et al.(2022) Elucidating anti-angiogenic potential of Rauwolfia serpentina: VEGFR-2 targeting based molecular docking study. Evidence-Based Complementary and Alternative Medicine,.In press:DOI: 10.1155/2021/6224666.

19. Perera WPTD, Dissanayake DMRK, Unagolla JM, De Silva RT, Bathige SDNK, Pahalagedara LR.(2022) Albumin grafted coaxial electrosparyed polycaprolactone-zinc oxide nanoparticle for sustained release and activity enhanced antibacterial drug delivery. RSC Adv.12(3):1718-27. doi: 10.1039/d1ra07847j.

20. Tabrez S, Khan AU, Mirza AA, Suhail M, Jabir NR, Zughaibi TA, et al.(2022) Biosynthesis of copper oxide nanoparticles and its therapeutic efficacy against colon cancer. Nanotechnology Reviews.11(1):1322-31. doi: 10.1515/ntrev-2022-0081.

21. Zughaibi TA, Mirza AA, Suhail M, Jabir NR, Zaidi SK, Wasi S, et al.(2022) Evaluation of Anticancer Potential of Biogenic Copper Oxide Nanoparticles (CuO NPs) against Breast Cancer. Journal of Nanomaterials.2022:e5326355. doi: 10.1155/2022/5326355.

22. Tabrez S, Khan A, Suhail M, Khan M, Zughaibi T, Hoque M.(2022) Biosynthesis of ZnO NPs from pumpkin seeds extract and elucidation of its anticancer activity against breast cancer. Nanotechnology Reviews.In press.

23. Anjum S, Hashim M, Malik SA, Khan M, Lorenzo JM, Abbasi BH, et al.(2021) Recent Advances in Zinc Oxide Nanoparticles (ZnO NPs) for Cancer Diagnosis, Target Drug Delivery, and Treatment. Cancers.13(18):4570. doi: 10.3390/cancers13184570.

13

24. El-Belely EF, Farag MMS, Said HA, Amin AS, Azab E, Gobouri AA, et al.(2021) Green Synthesis of Zinc Oxide Nanoparticles (ZnO-NPs) Using Arthrospira platensis (Class: Cyanophyceae) and Evaluation of their Biomedical Activities. Nanomaterials (Basel).11(1):95. doi: 10.3390/nano11010095.

25. Subramaniam H, Djearamane S, Tey LH, Wong LS, Gupta PK, Janakiraman AK.(2022) Potential of Zinc Oxide Nanoparticles as an Anticancer Agent: A Review. Journal of Experimental Biology and Agricultural Sciences.10(3):494-501. doi: 10.18006/2022.10(3).494.501.

26. Shait Mohammed MR, Ahmad V, Ahmad A, Tabrez S, Choudhry H, Zamzami MA, et al.(2021) Prospective of nanoscale metal organic frameworks [NMOFs] for cancer therapy. Seminars in Cancer Biology.69:129-39. doi: 10.1016/j.semcancer.2019.12.015.

27. Tabrez S, Khan AU, Hoque M, Suhail M, Khan MI, Zughaibi TA.(2022) Investigating the anticancer efficacy of biogenic synthesized MgONPs: An in vitro analysis. Frontiers in Chemistry.10.

28. Alharthy SA, Tabrez S, Mirza AA, Zughaibi TA, Firoz CK, Dutta M.(2022) Sugiol Suppresses the Proliferation of Human U87 Glioma Cells via Induction of Apoptosis and Cell Cycle Arrest. Evidence-Based Complementary and Alternative Medicine.2022:e7658899. doi: 10.1155/2022/7658899.

29. Gowd V, Ahmad A, Tarique M, Suhail M, Zughaibi TA, Tabrez S, et al.(2022) Advancement of cancer immunotherapy using nanoparticles-based nanomedicine. Seminars in Cancer Biology. doi: 10.1016/j.semcancer.2022.03.026.

30. Khan MS, Alomari A, Tabrez S, Hassan I, Wahab R, Bhat SA, et al.(2021) Anticancer Potential of Biogenic Silver Nanoparticles: A Mechanistic Study. Pharmaceutics.13(5):707. doi: 10.3390/pharmaceutics13050707.

31. Tabrez S, Hoque M, Suhail M, Khan MI, Zughaibi TA, Khan AU.(2022) Identification of anticancer bioactive compounds derived from Ficus sp. by targeting Poly[ADP-ribose]polymerase 1 (PARP-1). Journal of King Saud University - Science.34(5):102079. doi: 10.1016/j.jksus.2022.102079.

32. Cao Y, Dhahad HA, El-Shorbagy MA, Alijani HQ, Zakeri M, Heydari A, et al.(2021) Green synthesis of bimetallic ZnO–CuO nanoparticles and their cytotoxicity properties. Sci Rep.11(1):23479. doi: 10.1038/s41598-021-02937-1.

33. Berehu HM, S A, Khan MI, Chakraborty R, Lavudi K, Penchalaneni J, et al.(2021) Cytotoxic Potential of Biogenic Zinc Oxide Nanoparticles Synthesized From Swertia chirayita Leaf Extract on Colorectal Cancer Cells. Front Bioeng Biotechnol.9:788527. doi: 10.3389/fbioe.2021.788527.

34. Aalami AH, Mesgari M, Sahebkar A.(2020) Synthesis and Characterization of Green Zinc Oxide Nanoparticles with Antiproliferative Effects through Apoptosis Induction and MicroRNA Modulation in Breast Cancer Cells. Bioinorganic Chemistry and Applications.2020:e8817110. doi: 10.1155/2020/8817110.

14

35. Deka B, Baruah C, Babu A, Kalita P.(2022) Biological and Non-Conventional Synthesis of Zinc Oxide Nanoparticles (ZnO-NPs): Their Potential Applications. J Nanotechnol Nanomaterials.Volume 3(Issue 2):79-89. doi: 10.33696/Nanotechnol.3.034.

36. Gatou M-A, Lagopati N, Vagena I-A, Gazouli M, Pavlatou EA.(2023) ZnO Nanoparticles from Different Precursors and Their Photocatalytic Potential for Biomedical Use. Nanomaterials (Basel).13(1):122. doi: 10.3390/nano13010122.

37. Mandal AK, Katuwal S, Tettey F, Gupta A, Bhattarai S, Jaisi S, et al.(2022) Current Research on Zinc Oxide Nanoparticles: Synthesis, Characterization, and Biomedical Applications. Nanomaterials (Basel).12(17):3066. doi: 10.3390/nano12173066.

38. Ali A, Phull A-R, Zia M.(2018) Elemental zinc to zinc nanoparticles: is ZnO NPs crucial for life? Synthesis, toxicological, and environmental concerns. Nanotechnology Reviews.7(5):413-41. doi: 10.1515/ntrev-2018-0067.

39. Thatoi P, Kerry RG, Gouda S, Das G, Pramanik K, Thatoi H, et al.(2016) Photo-mediated green synthesis of silver and zinc oxide nanoparticles using aqueous extracts of two mangrove plant species, Heritiera fomes and Sonneratia apetala and investigation of their biomedical applications. Journal of Photochemistry and Photobiology B: Biology.163:311-8. doi: 10.1016/j.jphotobiol.2016.07.029.

40. Jafari A, Babajani A, Sarrami Forooshani R, Yazdani M, Rezaei-Tavirani M.(2022) Clinical Applications and Anticancer Effects of Antimicrobial Peptides: From Bench to Bedside. Frontiers in Oncology.12.

41. Navya PN, Kaphle A, Srinivas SP, Bhargava SK, Rotello VM, Daima HK.(2019) Current trends and challenges in cancer management and therapy using designer nanomaterials. Nano Converg.6(1):23. doi: 10.1186/s40580-019-0193-2.

42. Yang S-T, Liu J-H, Wang J, Yuan Y, Cao A, Wang H, et al.(2010) Cytotoxicity of Zinc Oxide Nanoparticles: Importance of Microenvironment. Journal of Nanoscience and Nanotechnology.10(12):8638-45. doi: 10.1166/jnn.2010.2491.

43. Mohammad F, Bwatanglang IB, Al-Lohedan HA, Shaik JP, Al-Tilasi HH, Soleiman AA.(2023) Influence of Surface Coating towards the Controlled Toxicity of ZnO Nanoparticles In Vitro. Coatings.13(1):172. doi: 10.3390/coatings13010172.

44. Ng CT, Yong LQ, Hande MP, Ong CN, Yu LE, Bay BH, et al.(2017) Zinc oxide nanoparticles exhibit cytotoxicity and genotoxicity through oxidative stress responses in human lung fibroblasts and Drosophila melanogaster. Int J Nanomedicine.12:1621-37. doi: 10.2147/IJN.S124403.

45. Thompson MW.(2022) Regulation of zinc-dependent enzymes by metal carrier proteins. Biometals.35(2):187-213. doi: 10.1007/s10534-022-00373-w.

46. Salari S, Neamati A, Tabrizi MH, Seyedi SMR.(2020) Green-synthesized Zinc oxide nanoparticle, an efficient safe anticancer compound for human breast MCF7 cancer cells. Applied Organometallic Chemistry.34(3):e5417. doi: 10.1002/aoc.5417.

15

47. Cheng J, Wang X, Qiu L, Li Y, Marraiki N, Elgorban AM, et al.(2020) Green synthesized zinc oxide nanoparticles regulates the apoptotic expression in bone cancer cells MG-63 cells. Journal of Photochemistry and Photobiology B: Biology.202:111644. doi: 10.1016/j.jphotobiol.2019.111644.

48. Carneiro BA, El-Deiry WS.(2020) Targeting apoptosis in cancer therapy. Nat Rev Clin Oncol.17(7):395-417. doi: 10.1038/s41571-020-0341-y.

49. Kc B, Paudel SN, Rayamajhi S, Karna D, Adhikari S, Shrestha BG, et al.(2016) Enhanced preferential cytotoxicity through surface modification: synthesis, characterization and comparative in vitro evaluation of TritonX-100 modified and unmodified zinc oxide nanoparticles in human breast cancer cell (MDA-MB-231). Chem Cent J.10:16. doi: 10.1186/s13065-016-0162-3.

50. Kang YJ, Kwon YH, Jang JY, Lee JH, Lee S, Park Y, et al.(2023) MHY2251, a New SIRT1 Inhibitor, Induces Apoptosis via JNK/p53 Pathway in HCT116 Human Colorectal Cancer Cells. Biomol Ther (Seoul).31(1):73-81. doi: 10.4062/biomolther.2022.044.

51. Boskabadi SH, Balanezhad SZ, Neamati A, Tabrizi MH.(2021) The green-synthesized zinc oxide nanoparticle as a novel natural apoptosis inducer in human breast (MCF7 and MDA-MB231) and colon (HT-29) cancer cells. Inorganic and Nano-Metal Chemistry.51(5):733-43. doi: 10.1080/24701556.2020.1808991.

52. Bai D-P, Zhang X-F, Zhang G-L, Huang Y-F, Gurunathan S.(2017) Zinc oxide nanoparticles induce apoptosis and autophagy in human ovarian cancer cells. Int J Nanomedicine.12:6521-35. doi: 10.2147/IJN.S140071.

53. Wang S-W, Lee C-H, Lin M-S, Chi C-W, Chen Y-J, Wang G-S, et al.(2020) ZnO Nanoparticles Induced Caspase-Dependent Apoptosis in Gingival Squamous Cell Carcinoma through Mitochondrial Dysfunction and p70S6K Signaling Pathway. International Journal of Molecular Sciences.21(5):1612. doi: 10.3390/ijms21051612.

54. Wang Y, Qi H, Liu Y, Duan C, Liu X, Xia T, et al.(2021) The double-edged roles of ROS in cancer prevention and therapy. Theranostics.11(10):4839-57. doi: 10.7150/thno.56747.

55. Aggarwal V, Tuli HS, Varol A, Thakral F, Yerer MB, Sak K, et al.(2019) Role of Reactive Oxygen Species in Cancer Progression: Molecular Mechanisms and Recent Advancements. Biomolecules.9(11):735. doi: 10.3390/biom9110735.

56. Alserihi RF, Mohammed MRS, Kaleem M, Khan MI, Sechi M, Sanna V, et al.(2022) Development of (−)-epigallocatechin-3-gallate-loaded folate receptor-targeted nanoparticles for prostate cancer treatment. Nanotechnology Reviews.11(1):298-311. doi: 10.1515/ntrev-2022-0013.

57. Karimzadeh MR, Soltanian S, Sheikhbahaei M, Mohamadi N.(2020) Characterization and biological activities of synthesized zinc oxide nanoparticles using the extract of Acantholimon serotinum. Green Processing and Synthesis.9(1):722-33. doi: 10.1515/gps-2020-0058.

58. Yue J, López JM.(2020) Understanding MAPK Signaling Pathways in Apoptosis. International Journal of Molecular Sciences.21(7):2346. doi: 10.3390/ijms21072346.

16

59. Wang X, Li Y, Li J, Li L, Zhu H, Chen H, et al.(2019) Cell-in-Cell Phenomenon and Its Relationship With Tumor Microenvironment and Tumor Progression: A Review. Frontiers in Cell and Developmental Biology.7.

60. NÚÑez JG, Pinheiro JS, Padilha GL, Garcia HO, Porta V, Apel MA, et al.(2020) Antineoplastic potential and chemical evaluation of essential oils from leaves and flowers of Tagetes ostenii Hicken. An Acad Bras Cienc.92(suppl 2):e20191143. doi: 10.1590/0001-3765202020191143.

61. Garrido-Urbani S, Vonlaufen A, Stalin J, De Grandis M, Ropraz P, Jemelin S, et al.(2018) Junctional adhesion molecule C (JAM-C) dimerization aids cancer cell migration and metastasis. Biochimica et Biophysica Acta (BBA) - Molecular Cell Research.1865(4):638-49. doi: 10.1016/j.bbamcr.2018.01.008.

62. Ovejero Paredes K, Díaz-García D, García-Almodóvar V, Lozano Chamizo L, Marciello M, Díaz-Sánchez M, et al.(2020) Multifunctional Silica-Based Nanoparticles with Controlled Release of Organotin Metallodrug for Targeted Theranosis of Breast Cancer. Cancers.12(1):E187. doi: 10.3390/cancers12010187.

63. Alafaleq NO, Alomari A, Khan MS, Shaik GM, Hussain A, Ahmed F, et al.(2022) Anticancer potential of gold nanoparticles (AuNPs) using a battery of in vitro tests. Nanotechnology Reviews.11(1):3292-304. doi: 10.1515/ntrev-2022-0502.

17

Figure legends:

Figure 1: Dose-dependent increase in cytotoxicity of ZnO NPs in PA-1 cell lines. The data are presented as a percentage of viable cells compared to the untreated control. Values are expressed as mean ± SD (n = 6) and analyzed by one-way ANOVA. ***, $P < 0.0001$.

Figure 2: Morphological changes in PA-1 cells treated with different concentrations of ZnO NPs (7.5, 10, and 12.5 µg/mL) for 24 hours.

Figure 3: AO/EtBr fluorescence pattern photographs of PA-1 cells treated with increasing concentrations of ZnO NPs (7.5, 10, and 12.5 µg/mL). Live (acridine stained), dead (EtBr stained), and early apoptotic (yellow stained) cells showed green, red, and yellow colors, respectively. Scale bar indicates 50 µm

Figure 4: Quantification percentage of ZnO NPs treated PA-1 apoptotic cells. Values are expressed as mean ± SD (n = 6) and analyzed by one-way ANOVA. **, $P < 0.001$; ***, $P < 0.0001$.

Figure 5: Fluorescence microscope images of ZnO NPs induced ROS production in PA-1 cells.

Figure 6: Quantitative fluorescence intensity showing induction in ROS production in response to different concentrations of ZnO NPs. Values are expressed as mean ± SD (n = 6) and analyzed by one-way ANOVA. ***, $P < 0.0001$.

Figure 7: Photomicrographs of cell adhesion after the treatment with ZnO NPs (7.5, 10, and 12.5 µg/mL) in PA-1 cells.

Figure 8: Microscopic images of *in-vitro* wound scratch healing process in PA-1 cells after the treatment with different concentrations of ZnO NPs.

18

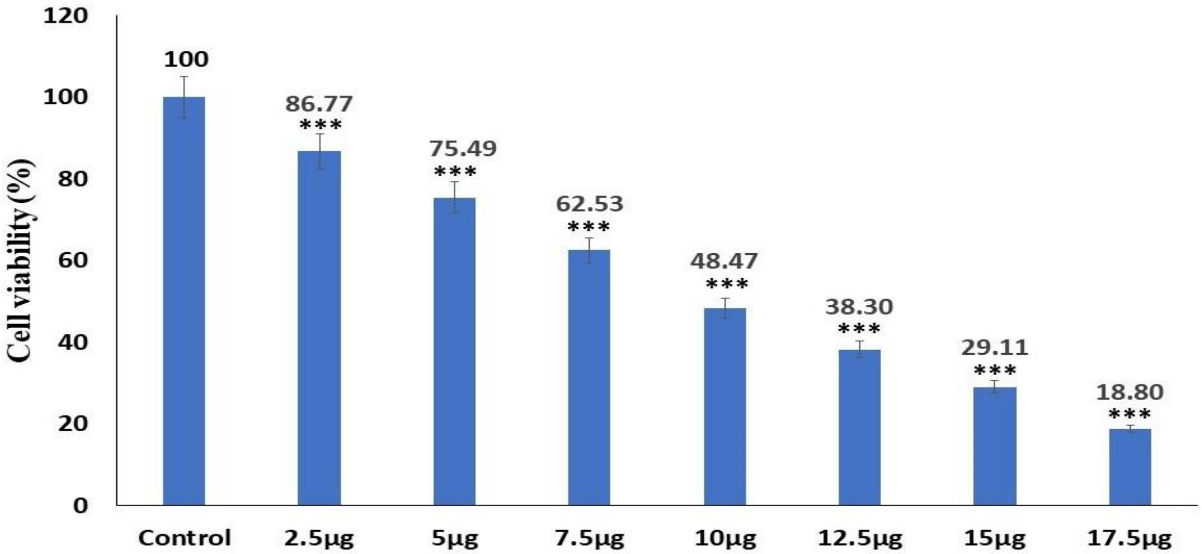
120
100
80
60
40
20
0
Cell viability (%)
100
86.77
75.49
62.53
48.47
38.30
29.11
18.80
***
Control
2.5µg
5µg
7.5µg
10µg
12.5µg
15µg
17.5µg

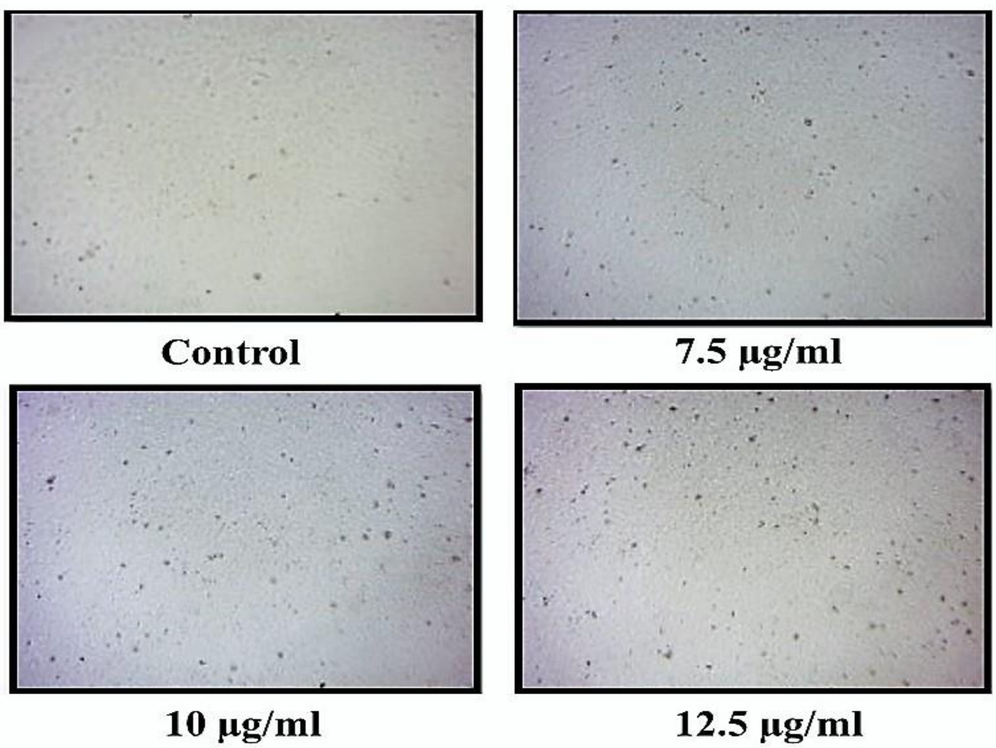
Control
7.5 µg/ml
10 µg/ml
12.5 µg/ml

19

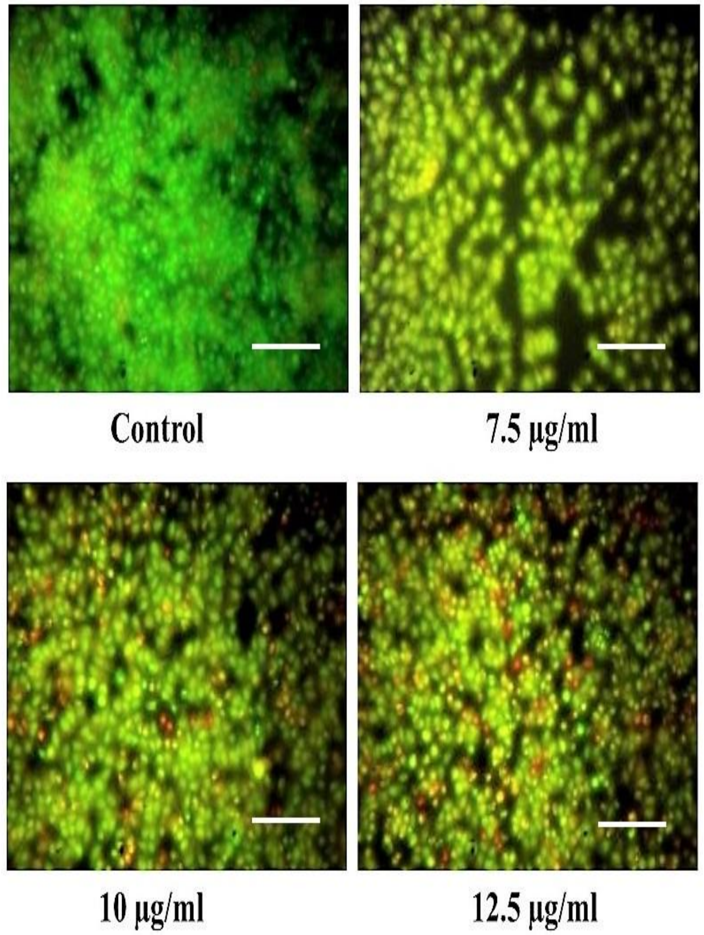
Control
7.5 µg/ml
10 µg/ml
12.5 µg/ml

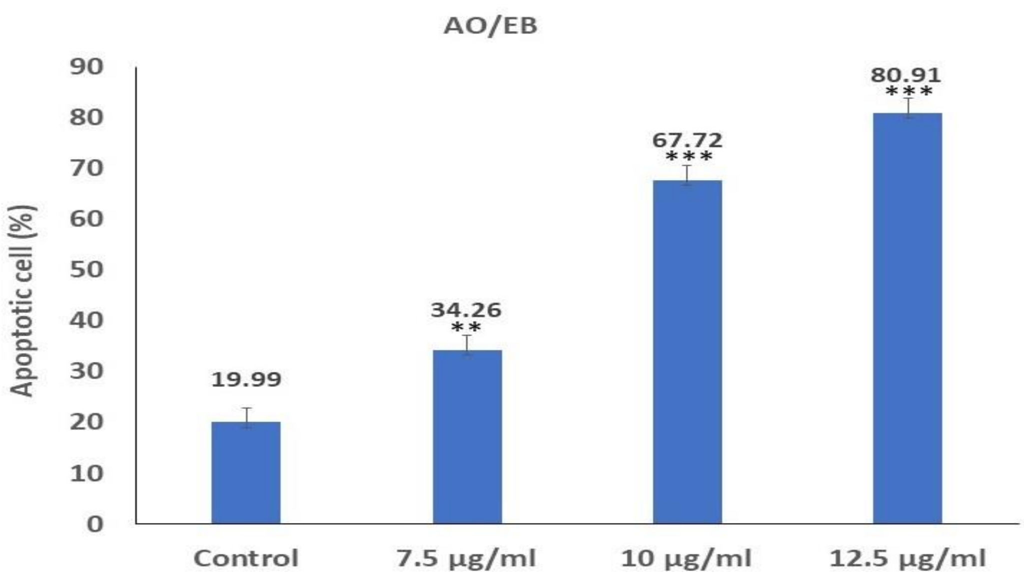
AO/EB
Apoptotic cell (%)
0
10
20
30
40
50
60
70
80
90
19.99
34.26
**
67.72
***
80.91
***
Control
7.5 µg/ml
10 µg/ml
12.5 µg/ml

20

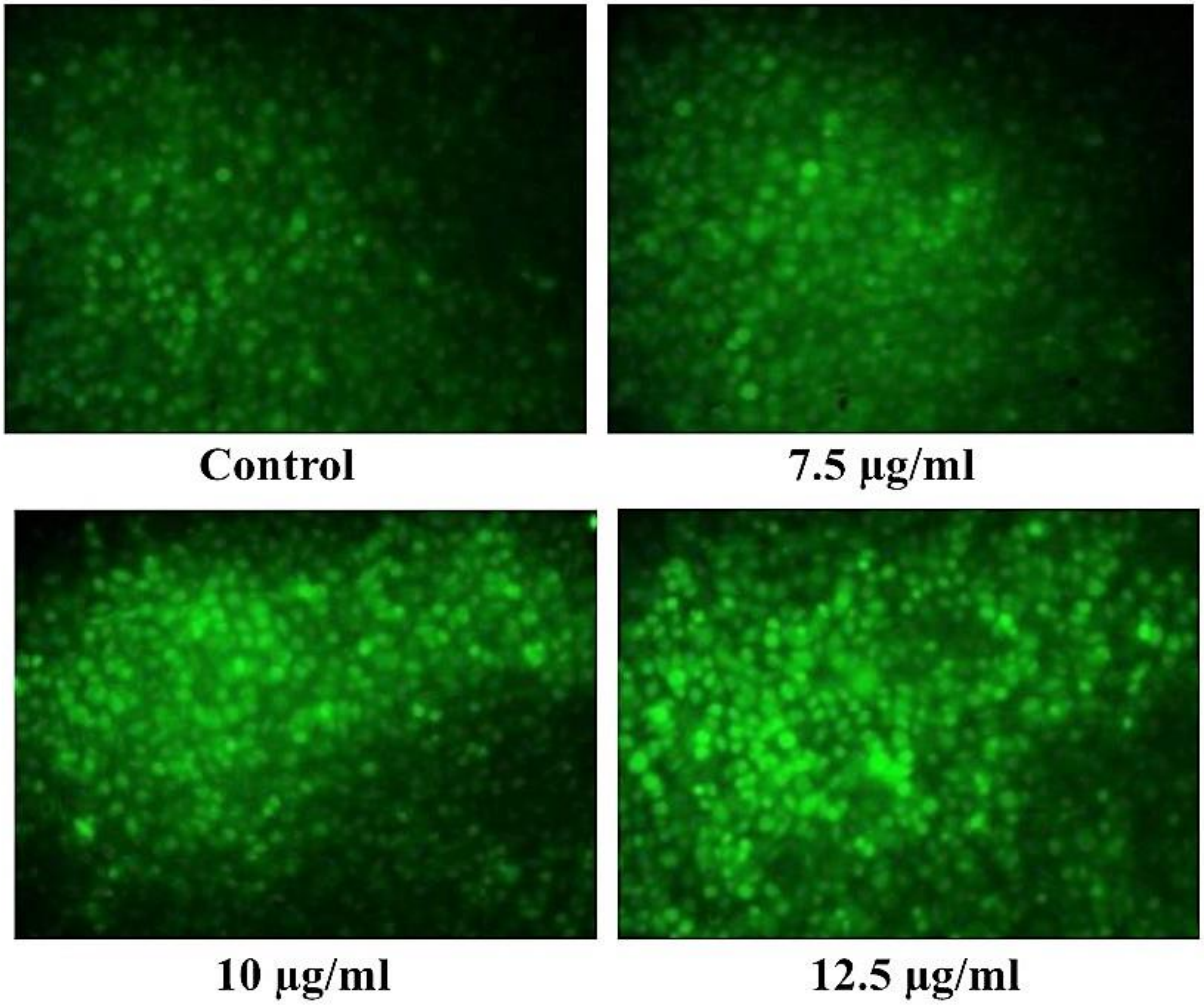

21

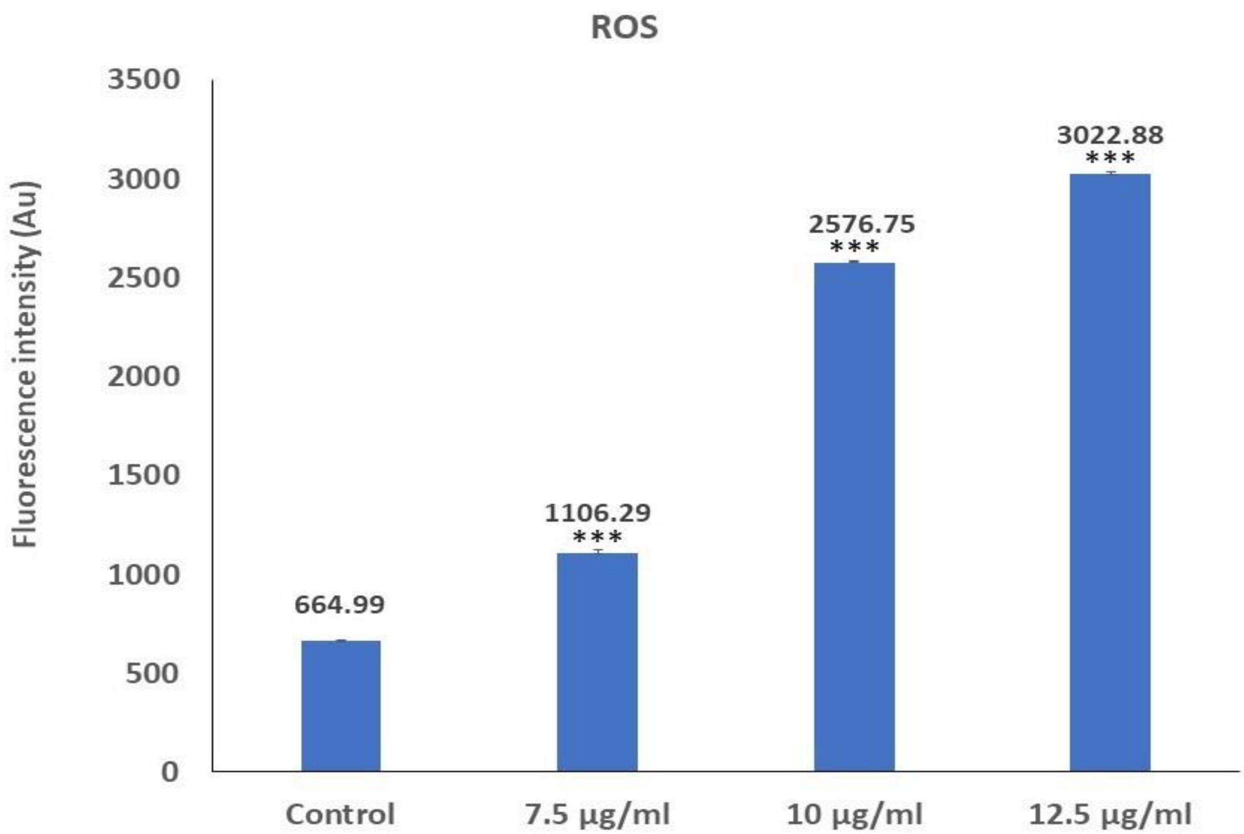
ROS
Fluorescence intensity (Au)
3500
3000
2500
2000
1500
1000
500
0
664.99
1106.29
***
2576.75
***
3022.88
***
Control
7.5 µg/ml
10 µg/ml
12.5 µg/ml

22

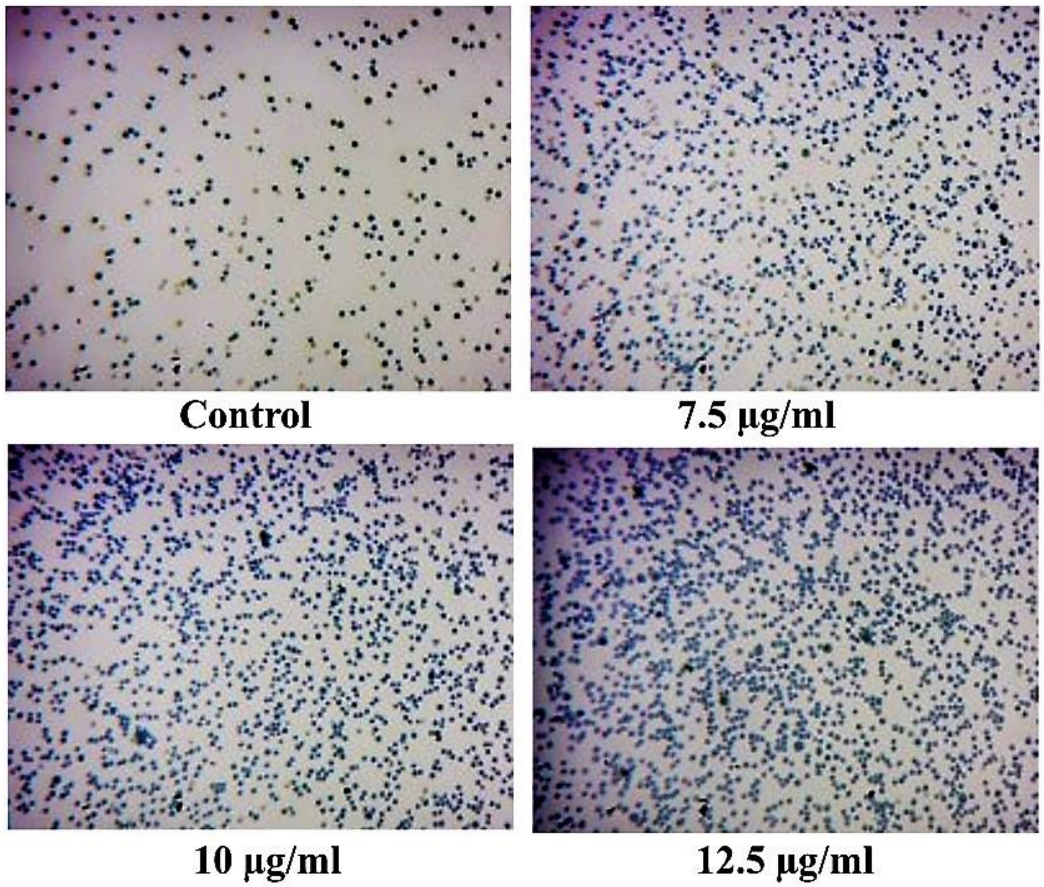
Control
7.5 µg/ml
10 µg/ml
12.5 µg/ml

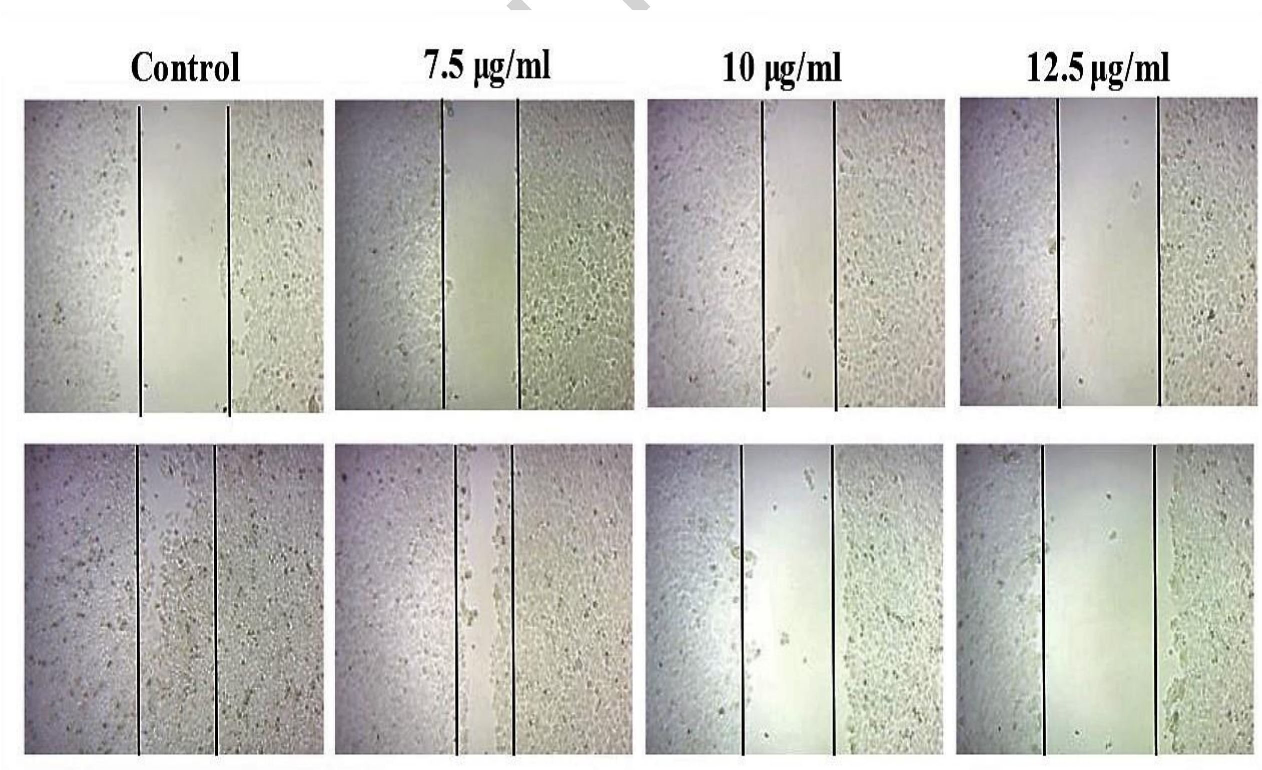
Control
7.5 µg/ml
10 µg/ml
12.5 µg/ml

23